Research Article | Vol. 25, No. 13 | 26 Jun 2017 | OPTICS EXPRESS 15539
Optics EXPRESS

Dispersive heterodyne probing method for laser frequency stabilization based on spectral hole burning in rare-earth doped crystals

O. Gobron,[1,2] K. Jung,[1,3] N. Galland,[4] K. Predehl,[1,5] R. Le Targat,[1] A. Ferrier,[6,7] P. Goldner,[6] S. Seidelin,[4,8] and Y. Le Coq[1,*]

[1] *LNE-SYRTE, Observatoire de Paris, PSL Research University, CNRS, Sorbonne Universités, UPMC Univ. Paris 06, 61 avenue de l'Observatoire, 75014 Paris, France*
[2] *Currently with Department of Physics, Technical University of Denmark, 2800 Kongens Lyngby, Denmark*
[3] *Currently with Samsung Electro-Mechanics, 16674 Suwon, South Korea*
[4] *Univ. Grenoble Alpes and CNRS, Inst. NEEL, F-38042 Grenoble, France*
[5] *Currently with Fraunhofer IPM, Heidenhofstr. 8, D-79110, Freiburg, Germany*
[6] *PSL Research University, Chimie ParisTech, CNRS, Institut de Recherche de Chimie Paris, 75005, Paris, France*
[7] *Sorbonne Universités, UPMC Université Paris 06, 75005, Paris, France*
[8] *Institut Universitaire de France, 103 Boulevard Saint-Michel, F-75005 Paris, France*
[*] *yann.lecoq@obspm.fr*

Abstract: Frequency-locking a laser to a spectral hole in rare-earth doped crystals at cryogenic temperature has been shown to be a promising alternative to the use of high finesse Fabry-Perot cavities when seeking a very high short term stability laser (M. J. Thorpe et al., Nature Photonics **5**, 688 (2011)). We demonstrate here a novel technique for achieving such stabilization, based on generating a heterodyne beat-note between a master laser and a slave laser whose dephasing caused by propagation near a spectral hole generate the error signal of the frequency lock. The master laser is far detuned from the center of the inhomogeneous absorption profile, and therefore exhibits only limited interaction with the crystal despite a potentially high optical power. The demodulation and frequency corrections are generated digitally with a hardware and software implementation based on a field-programmable gate array and a Software Defined Radio platform, making it straightforward to address several frequency channels (spectral holes) in parallel.

OCIS codes: (120.3930) Metrological instrumentation; (120.2230) Fabry-Perot; (140.3425) Laser stabilization; (160.5690) Rare-earth-doped materials.

References and links

1. M. Schioppo, R. C. Brown, W. F. McGrew, N. Hinkley, R. J. Fasano, K. Beloy, T. H. Yoon, G. Milani, D. Nicolodi, J. A. Sherman, N. B. Phillips, C. W. Oates, and A. D. Ludlow, "Ultrastable optical clock with two cold-atom ensembles," Nat. Photonics **11**, 48-52 (2017).
2. R. Tyumenev, M. Favier, S. Bilicki, E. Bookjans, R. Le Targat, J. Lodewyck, D. Nicolodi, Y. Le Coq, M. Abgrall, J. Guéna, L. De Sarlo, and S. Bize, "Comparing a mercury optical lattice clock with microwave and optical frequency standards," New. J. Phys. **18**, 113002 (2016).
3. C. Lisdat, G. Grosche, N. Quintin, C. Shi, S.M.F. Raupach, C. Grebing, D. Nicolodi, F. Stefani, A. Al-Masoudi, S. Dörscher, S. Häfner, J.-L. Robyr, N. Chiodo, S. Bilicki, E. Bookjans, A. Koczwara, S. Koke, A. Kuhl, F. Wiotte, F. Meynadier, E. Camisard, M. Abgrall, M. Lours, T. Legero, H. Schnatz, U. Sterr, H. Denker, C. Chardonnet, Y. Le Coq, G. Santarelli, A. Amy-Klein, R. Le Targat, J. Lodewyck, O. Lopez, and P.-E. Pottie, "A clock network for geodesy and fundamental science," Nat. Commun. **7**, 12443 (2016).
4. I. Ushijima, M. Takamoto, M. Das, T. Ohkubo, and H. Katori, "Cryogenic optical lattice clocks," Nat. Photonics **9**, 185-189 (2015).
5. T. L. Nicholson, S. L. Campbell, R. B. Hutson, G. E. Marti, B. J. Bloom, R. L. McNally, W. Zhang, M. D. Barrett, M. S. Safronova, G. F. Strouse, W. L. Tew, and J. Ye, "Systematic evaluation of an atomic clock at $2x10^{-18}$ total uncertainty," Nature Commun. **6**, 6896 (2015).

#295072 https://doi.org/10.1364/OE.25.015539
Journal © 2017 Received 5 May 2017; revised 19 Jun 2017; accepted 19 Jun 2017; published 23 Jun 2017

Optics EXPRESS

6. S. Häfner, S. Falke, C. Grebing, S. Vogt, T. Legero, M. Merimaa, C. Lisdat, and U. Sterr, "$8x10^{-17}$ fractional laser frequency instability with a long room-temperature cavity," Opt. Lett. **40**, 2112-2115 (2015).
7. B. P. Abbott (LIGO Scientific Collaboration and Virgo Collaboration), "Observation of Gravitational Waves from a Binary Black Hole Merger," Phys. Rev. Lett. **116**, 061102 (2016).
8. For gravitational wave detectors in space, see https://www.elisascience.org/
9. X. Xie, R. Bouchand, D. Nicolodi, M. Giunta, W. Hänsel, M. Lezius, A. Joshi, S. Datta, C. Alexandre, M. Lours, P.-A. Tremblin, G. Santarelli, R. Holzwarth, and Y. Le Coq, "Photonic microwave signals with zeptosecond-level absolute timing noise," Nat. Photonics **11**, 44-47 (2017).
10. K. Numata, A. Kemery, and J. Camp, "Thermal-Noise Limit in the Frequency Stabilization of Lasers with Rigid Cavities," Phys. Rev. Lett. **93**, 250602 (2004).
11. Note that the linewidth of the transmission peak does not impact the limitation due to thermal agitation, but a narrow peak reduces strongly the impact of a wide group of technical noise (detection noise, effect of parasitic reflexions, residual amplitude modulation in a Pound-Drever-Hall (PDH) servo loop, etc.
12. S. Häfner, S. Falke, C. Grebing, S. Vogt, T. Legero, M. Merimaa, C. Lisdat, and U. Sterr, "A second generation of low thermal noise cryogenic silicon resonators," Opt. Lett. **40**, 2112-2115 (2015).
13. G. Cole, W. Zhang, M. Martin, J. Ye, and M. Aspelmeyer, "Tenfold reduction of Brownian noise in high-reflectivity optical coatings," Nat. Photonics **7**, 644-650 (2013).
14. E. Wiens, Q.-F. Chen, I. Ernsting, H. Luckmann, U. Rosowski, A. Nevsky, and S. Schiller, "Silicon single-crystal cryogenic optical resonator," Opt. Lett. **39**, 3242-3245 (2014).
15. B. Julsgaard, A. Walther, S. Kröll, and L. Rippe, "Understanding laser stabilization using spectral hole burning," Opt. Express **15**, 11445-11465 (2007).
16. M. J. Thorpe, L. Rippe, T. M. Fortier, M. S. Kirchner, and T. Rosenband, "Frequency stabilization to $6x10^{-16}$ via spectral-hole burning," Nat. Photonics **5**, 688-693 (2011).
17. R. Yano, M. Mitsunaga, and N. Uesugi, "Ultralong optical dephasing time in Eu^{3+}:Y_2SiO_5," Opt. Lett. **16**, 1884-1886 (1991).
18. R. W. Equall, Y. Sun, R. L. Cone, and R. M. Macfarlane, "Ultraslow Optical Dephasing in Eu^{3+}:Y_2SiO_5," Phys. Rev. Lett. **72**, 2179 (1994).
19. F. Könz, Y. Sun, C. W. Thiel, R. L. Cone, R. W. Equall, R. L. Hutcheson, and R. M. Macfarlane, "Temperature and concentration dependence of optical dephasing, spectral-hole lifetime, and anisotropic absorption in Eu^{3+}:Y_2SiO_5," Phys. Rev. B **68**, 085109 (2003).
20. Q.-F. Chen, A. Troshyn, I. Ernsting, S. Kayser, S. Vasilyev, A. Nevsky, and S. Schiller, "Spectrally Narrow, Long-Term Stable Optical Frequency Reference Based on a Eu^{3+}:Y_2SiO_5 Crystal at Cryogenic Temperature," Phys. Rev. Lett. **107**, 223202 (2011).
21. M. J. Thorpe, D. R. Leibrandt, and T. Rosenband, "Shifts of optical frequency references based on spectral-hole burning in Eu^{3+}:Y_2SiO_5," New J. Phys. **15**, 033006 (2013).
22. S. Cook, T. Rosenband, and D. R. Leibrandt, "Laser-Frequency Stabilization Based on Steady-State Spectral-Hole Burning in Eu^{3+}:Y_2SiO_5," Phys. Rev. Lett. **114**, 253902 (2015).
23. D. Leibrandt, M. Thorpe, C.-W. Chou, T. Fortier, S. Diddams, and T. Rosenband, "Absolute and Relative Stability of an Optical Frequency Reference Based on Spectral Hole Burning in Eu^{3+}:Y_2SiO_5," Phys. Rev. Lett. **111**, 237402 (2013).
24. L. S. Ma, P. Junger, J. Ye, and J. L. Hall, "Delivering the same optical frequency at two places: accurate cancellation of phase noise introduced by an optical fiber or other time-varying path," Opt. Lett. **19**, 1777-1779 (1994).
25. The difference in powers mostly arises from the different efficiencies of the fiber coupling at 1160 nm.
26. D. Nicolodi, B. Argence, W. Zhang, R. Le Targat, G. Santarelli, and Y. Le Coq, "Spectral purity transfer between optical wavelengths at the 10^{-18} level," Nat. Photonics **8**, 219-223 (2014).
27. D. Leibrandt (National Institute of Standards and Technology) and W. Zhang (JILA), Boulder, Colorado (personal communication, 2016).
28. A. Ferrier, B. Tumino, and P. Goldner, "Variations in the oscillator strength of the $^7F_0 - ^5D_0$ transition in single crystals," J. Lumin. **170**, 406-410 (2016).
29. http://gnuradio.org/
30. B. Argence, E. Prevost, T. Lévèque, R. Le Goff, P. Lemonde, S. Bize, and G. Santarelli, "Prototype of an ultra-stable optic cavity for space applications," Opt. Express, **20**, 25409-25420 (2012).
31. J. Lodewyck, S. Bilicki, E. Bookjans, J.-L. Robyr, C. Shi, G. Vallet, R. Le Targat, D. Nicolodi, Y. Le Coq, J. Guéna, M. Abgrall, P. Rosenbusch, and S. Bize, "Optical to microwave clock frequency ratios with a nearly continuous strontium optical lattice clock," Metrologia **53**, 1123-1130 (2016).
32. K. Mølmer, Y. Le Coq, and S. Seidelin, "Dispersive coupling between light and a rare-earth-ion-doped mechanical resonator," Phys. Rev. A **94**, 053804 (2016).

1. Introduction

Continuous wave lasers with ultra-high stability and low optical phase noise are of prime importance in many high precision measurement experiments. They constitute, in particular,

Optics EXPRESS

an essential building block for the development of state-of-the-art optical lattice clocks [1–6], gravitational wave detectors [7, 8] or opto-electronic generation of ultra-low phase noise microwave signals [9]. The most stable lasers are currently realized by making a tight frequency lock to the transmission peak of a high-finesse (typically 10^5-10^6) Fabry-Perot cavity maintained in a carefully designed and controlled environment (vacuum chambers with 10^{-7} mbar residual pressure or lower, reduced thermal expansion materials and design, high temperature-stability at the μK level or lower, vibration isolation platforms and low vibration sensitivity design, etc.). Several decades of efforts aiming at reducing the effect of technical perturbations have led nowadays to systems with stabilities imposed by the fundamental limitation arising from thermal agitation of the atoms that constitute the Fabry-Perot cavity [10]. For a 10 cm long cavity using amorphous glass at 300 K, exhibiting transmission peaks of several kHz linewidth [11], this corresponds to 10^{-15} fractional frequency stability (or slightly lower) for a timescale of around 1 second. Various strategies are currently being explored to circumvent the limitation due to thermal agitation, including the use of larger cavities [6], crystalline materials for spacers and mirrors [12], or for coatings [13], as well as operation at cryogenic temperatures [14].

All these strategies rely on improved Fabry-Perot cavities. An alternative approach is to frequency lock a laser to narrow spectral features previously photo-imprinted in rare-earth doped crystals by spectral-hole burning [15]. Spectral features as narrow as 1 kHz have thus been observed in Eu^{3+}:Y_2SiO_5 crystals [16], with photon-echo experiments indicating the possibility to achieve structures as narrow as a few 100 Hz [17, 18]. In this technique, a laser pre-stabilized to a Fabry-Perot cavity (a stability of 10^{-12} at 0.1-1 second is sufficient, considering the typical widths of the spectral features) is used to photo-imprint one or several narrow spectral holes in an inhomogenously broadened absorption spectrum by selectively pumping the resonant rare-earth atoms into a dark long-lived state. In the case of Europium atoms in a Yttrium orthosilicate matrix (Eu^{3+}:Y_2SiO_5), the lifetime of the dark state can be several days (at 2 K) [19]. In a second step, the same laser can be frequency locked to these spectral features, which leads to substantial improvement in terms of stability compared to the exclusively pre-stabilized laser. Short term stabilities of 6×10^{-16} between 2 and 10 s have been demonstrated with this technique [16], as well as frequency drift rates as low as 5 mHz/s on long time scales [20]. The sensitivity of such an optical frequency reference to various external parameters has been measured [21] and a method for truly continuous operation, despite the unavoidable degradation of spectral holes in the presence of a laser probe (which causes hole overburning), has been demonstrated [22]. The ultimate limitation of such a technique is yet to be explored in terms of stability, but as the reference crystal is by definition kept at cryogenic temperature (4 K), and exhibits a Young's modulus much higher than that of amorphous glass at room temperature, the thermo-mechanical limit is expected to be much lower than that of standard room-temperature Fabry-Perot cavity based systems.

In the present work, we describe a novel method for generating an error signal suitable for frequency locking a laser to a spectral hole. Methods previously used for frequency locking to spectral holes include side-of-fringe locking (alternating left and right sides in side-of-fringe locking to remove effects of probe laser amplitude fluctuations) [16], as well as a Pound-Drever-Hall (PDH) method utilizing an electro-optic modulator to create sidebands on the probing laser prior to propagation through the crystal [21, 23]. In our method, the frequency offset information is, similarly to the PDH method, encoded in the phase of the probe laser. This phase is modified during the propagation through a narrow and hence highly dispersive spectral hole. However, unlike in the PDH method, the optical phase is measured by the beat frequency against a single sideband, sufficiently frequency detuned to be only marginally influenced by the absorption spectrum. Furthermore, the beat note signal is fully digitized by fast analog to digital converters (ADC) and processed in a Field Programmable Gate Arrays (FPGA) unit and a control computer using an open-source Software Defined Radio (SDR) platform, allowing

Optics EXPRESS

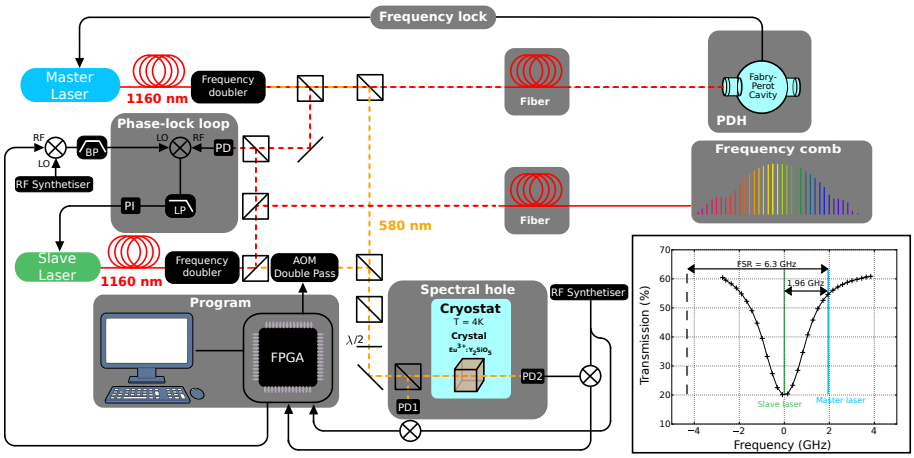

Fig. 1. Schematics of the optical part of the experimental setup (LP: Low-pass filter, BP: Band-pass filter, PI: Proportional-Integral corrector, FPGA: Field Programmable Gate Arrays, AOM: Acousto-optic modulator). The graph in the insert displays the transmission of the inhomogeneously broadened profile of the dopants in the crystal.

fast prototyping and testing of the data processing and of the feedback method. As a proof-of-principle, we demonstrate this method by effectively locking a laser pre-stabilized onto a reference cavity exhibiting $\sim 10^{-13}$ stability level near 1 s timescale to a narrow (4 kHz linewidth) spectral hole, for several hours. The resulting laser exhibits a stability of $\sim 2 \times 10^{-14}$ at 1 s, about an order of magnitude improvement over the solely pre-stabilized laser. Furthermore, the fully digital heterodyne method has the potential to multi-hole parallel probing which holds promise to improve detection signal to noise ratio in future work.

2. Optical setup

The optical setup of the experiment is represented in Fig. 1. The optical system is based on two extended cavity diode lasers (ECDL), referred to as Master and Slave, at 1160 nm (Toptica DLPro), delivering 65 mW each. Both lasers are fiber coupled and frequency doubled in PPLN waveguides with free space outputs (NTT Electronics) to reach 580 nm, corresponding to the wavelength of absorption of the ${}^7F_0 - {}^5D_0$ transition in Eu^{3+}:Y_2SiO_5. The master laser at 1160 nm is frequency locked by the PDH method to a commercial reference cavity (Stable Laser Systems). Both the diode laser current and a piezo actuator acting on the external cavity length are used for feedback, with a bandwidth around 500 kHz. A noise canceled fiber optical link [24] connects the master laser ECDL to the cavity itself, as it stays in a separate acoustically-isolated chamber on an active vibration-isolation platform (TS-150 from The Table Stable Ltd.). After the optical frequency doublers, 8.8 mW of 580 nm light is obtained from the master laser, and 4.5 mW for the slave laser [25]. Furthermore, due to finite efficiency, a part of the 1160 nm light that is sent to the doublers is not frequency doubled and is available at 1160 nm at the doublers outputs where they can be separated from the 580 nm light by dichroic mirrors. A part (1 mW) of this 1160 nm light from the slave laser is sent (via a noise canceled optical fiber) to an erbium-doped fiber based optical frequency comb, which can be used for characterization, or, in the future, for transfer of spectral purity to or from other ultrastable lasers operating at different wavelengths [26] (including some lasers used for probing optical clock transitions). Another part of the 1160 nm light from the master laser is used to make a beatnote signal with the similar output of the slave frequency doubler. This beatnote signal (typically at around 900 MHz) is demodulated to baseband in a double balanced mixer (DBM) with a synthesized pure tone signal

Optics EXPRESS

near 900 MHz (obtained by the mixing of a fixed 980 MHz signal from a synthesizer and a tunable ≈80 MHz signal from the SDR platform) and low-pass filtered to generate an error signal suitable for offset phase locking the slave laser onto the master laser. A proportional and double integrator corrector realizes the phase locking, by acting on the current and piezo actuator of the slave laser, with a bandwidth of typically 500 kHz.

Note that using the outputs of the frequency doublers at 1160 nm instead of part of the input insures that excess phase noise in the optical fiber that seeds the doublers is also eliminated with the phase lock loop. In this setup, the slave laser at 580 nm benefits from the spectral purity and stability imposed by the reference cavity, but with an offset frequency that can be tuned (continuously if necessary) by changing the RF frequency of the synthesized signals applied to the DBM. Further control of the 580 nm laser field generated by the slave laser is provided by an acousto-optic modulator (AOM, central frequency at 80 MHz) used in double-pass configuration. By choosing accordingly the reference Fabry-Perot cavity mode onto which the master laser is frequency locked, and the frequency difference between the master and the slave lasers, we ensure that the master laser at 580 nm is situated on the far wing of the ~ 2 GHz wide inhomogenously broadened absorption spectrum, while the slave laser at 580 nm is positioned near the center of this profile (see inset in Fig. 1.)

The 580 nm light from the master and slave lasers are then recombined in a polarizing beam splitter, pass through a short (5 cm) single mode fiber (for optimal mode matching), a second polarizer and a $\lambda/2$ waveplate to obtain identical and tunable polarizations. Lenses are used to adjust the beam diameter to about 5 mm. A third polarizing beam splitter then allows splitting the combined beam in two parts, one impinging directly on a fast silicon photodiode (EOT 2030A), the other passing through the crystal after polarization tuning via a final $\lambda/2$ waveplate, before being also photodetected. This last waveplate allows to tune the polarization for optimum absorption in the crystal.

3. Crystal and cryostat

The cryostat we use to maintain the crystal near 4 K is a commercial system based on a Gifford-Macmahon closed cooling cycle with a vibration isolation stage between the cooler and the science chamber used to reduce the impact of the vibrations onto the sample (Montana Instruments Cryostation). It was observed however that vibrations, synchronous to the cooling cycle, were producing substantial perturbations of the spectral feature when probing spectral holes of a few kHz linewidth (temperature below 6 K). A possible solution that has been applied by other groups to solve this problem involves probing synchronously with the cooling cycle and only at "quiet" moments during the cycle. This solution is not suitable here as we require continuous operation for many hours and definitely no interruption of operation one or more times per cycle of the cryo-cooler. Another possibility involves drastic modifications of the cryostat to isolate even further the science chamber from the cooler, basically placing these two parts on separate tables [27]. Instead, we applied a different solution, outlined in the following, which is simpler, and that proved effective up to this point, although we do believe further work may be necessary to reach ultimate stability.

The crystal is mounted in a cylindrical copper block as shown in Fig. 2(a). This cylinder is positioned on 3 beryllium-copper springs (1 cm long, 4 mm diameter) on the cold head of the cryostat. Thermal contact between the mounting block and the cold head is realized with three groups of five annealed copper stripes (5 mm broad, 4 cm long, 200 μm thick each). Temperatures as low as 4 K could be reached in the vicinity of the crystal (as measured with calibrated thermistors). This extra stage of vibration isolation proved sufficient to remove the residual mechanical perturbation from the cooling cycle and observe spectral holes with 4 kHz linewidth for temperatures below 6 K, as shown in Fig. 2(b).

The crystal is a $8 \times 8 \times 6$ mm parallelepiped of yttrium orthosilicate, Y_2SiO_5, with the two

Optics EXPRESS

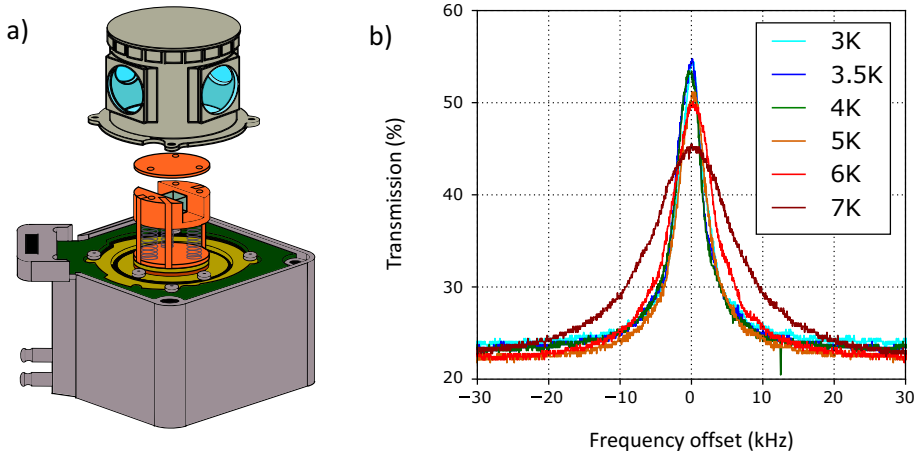

Fig. 2. a) Schematics of the cryostat mount of the Eu^{3+}:Y_2SiO_5 crystal that prevents residual vibrations during the cooling cycle to strongly disturb atomic transition frequencies. The crystal mount itself is standing on three beryllium-copper springs that provide an extra vibration isolation stage. Thermal contact is realized by three groups of five annealed copper stripes. b) Transmission spectrum of a spectral hole corresponding to different temperatures of the crystal, using the cryostat mount depicted in a). The transmission percentage indicated takes into account the losses which are independent of the atomic absorption, caused by interfaces devoid of anti-reflection coating (the faces of the crystal in particular).

largest faces polished for optical beam propagation. The crystal was grown by Czochralski process with 0.1% europium doping. After x-ray orientation, it was cut and polished so that the optical beam can propagate along the crystallographic *b* axis, and the two other faces were oriented along the principal dielectric axes D1 and D2. The lasers were tuned to the $^7F_0 - ^5D_0$ transition of site 1 at 580.038 nm (vacuum) and polarized along the D1 axis for maximal absorption [28]. The two polished faces were however set with a small relative angle (2 degrees) to prevent parasitic Fabry-Perot cavities build-up. The crystal is mounted in the cylindrical copper block inside a square groove and thermally contacted with silver lacquer.

4. Digital processing

In a first step, long ($\sim$ 120 ms) pulses of the slave laser at relatively high optical intensity ($\sim$ 20 μW.cm^{-2}) are applied to burn a spectral hole near the center of the inhomogeneously broadened absorption spectrum. If necessary, several holes can also be burned by repeating the pulse sequence for different optical frequencies, adapting the frequency applied to the double pass AOM as required.

The absorption profile of the spectral hole is subsequently probed in order to extract the value of a possible frequency offset between the hole and the slave laser. This is achieved by a dispersive technique: while propagating through a narrow absorbing spectral feature, the slave laser at 580 nm experiences a phase shift which is detected by a beatnote signal with the master laser at 580 nm. As the master laser is detuned to be on the far wing of the absorption spectrum, it is only marginally impacted by dispersion due to the interaction with the ions in the crystal. Moreover, due to its high power, the master laser immediately pumps ions around its frequency into dark, non-resonant states, limiting even further dispersive effects. Consequently, this laser constitutes a good optical phase reference. Furthermore, it can be operated at a relatively high power

Optics EXPRESS

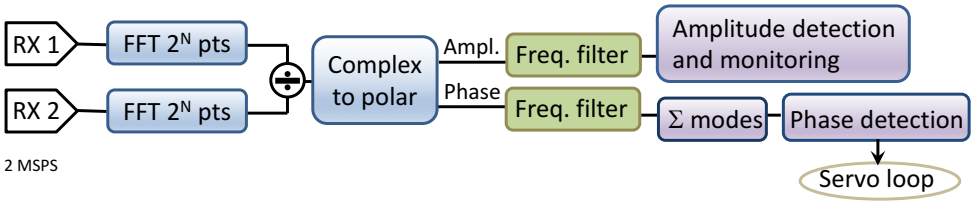

Fig. 3. Digitalization and data processing chart. The input data channels are streamed at a rate of 2×10^6 samples per seconds (2 MSPS). The data channels are processed by vectors of 2^N samples each (here, typically $N \geq 7$). The vectors are processed by Fast Fourier Transform algorithm before the two channels are divided in the Fourier domain. The resulting vector is separated in amplitude and phase components before being processed by a programmable frequency filter (which amounts to a multiplication by a filtering vector in the Fourier domain), which extracts data only at frequency modes in which signal is expected. The phase vector data is then summed, in order to combine the information from all the frequency channels in which signal is expected, and the resulting signal is used as an error signal for the servo loop maintaining the slave laser at resonance with the spectral hole(s).

without over-burning the narrow spectral feature used for the frequency lock. This facilitates the photodection of the beatnote by reducing the required amplification of the signal, and improves the thermal noise limited signal-to-noise ratio. This is in stark contrast with the classic PDH method, where sidebands substantially smaller than the probe beam are generated by means of an electro-optic modulator and serve as an optical reference for measuring the dephasing of the probe beam after demodulation. In this scenario, the sidebands, whose frequencies are much closer to the narrow spectral hole, do not provide as much beatnote signal amplitude as they are substantially smaller in amplitude than the probe beam, and are typically much closer to the spectral hole, therefore producing some hole burning of their own after a while.

In our case, we typically use 100 nW and a beam cross section of 0.5 cm^2 for the probe (slave) beam, and 1 mW in 0.5 cm^2 for the master laser, allowing continuous operation for several hours, even without the repumping processes used in [22] by Cook et al. The beat note is detected by two photodiodes. The two signals are amplified, down-converted to approximately 10 MHz by use of triple-balanced mixers (Marki T3) and a common mode synthesizer at 1.95 GHz, bandpass filtered and digitized at 200×10^6 samples per second (200 MSPS).

The digitalization and data processing is realized by use of a Software Defined Radio platform (SDR, Ettus research X310 with Basix Rx and Basix Tx daughter boards), utilizing the open source framework GNU Radio [29] in the control computer. The SDR two emission ports control, respectively, the double pass AOM and the offset-phase lock between the master and the slave laser. The flow diagram is depicted in Fig. 3. The two reception ports receive signals originating from the two photodetectors PD1 and PD2 (see Fig. 1) after their signals are down-converted to near 10 MHz. After analog to digital conversion, the two data channels are digitally down-converted to baseband by a FPGA and the In-phase (I) and Quadrature-phase (Q) are streamed to the control computer at a 2 MSPS rate in the form of complex data samples $I + iQ$. In the computer, the two streams of complex data are divided (PD2/PD1) in the Fourier plane (using the Fast Fourier Transform algorithm), bandpass filtered at the expected frequency of the signal, and the phase and amplitude of the beatnote is extracted. A major advantage of this topology is the straightforward reconfiguration to probe different frequency channels, either successively or simultaneously, which is necessary for interrogating multiple spectral holes. With 2 MSPS input rate, accessing frequency channels within the range of ±1 MHz is possible. After this

Optics EXPRESS

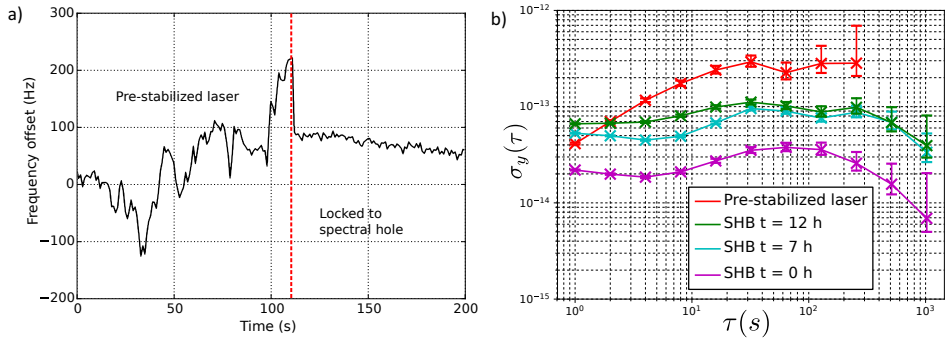

Fig. 4. a) Comparison between the frequency offset as a function of time of the laser being exclusively pre-stabilized (left side of the red dashed line) and being locked to a spectral hole (right side of the red dashed line). b) Allan variance of the exclusively pre-stabilized laser (red curve), and locked to a spectral hole obtained after a time delay of 0, 7 and 12 hours (purple, turquoise and green curve) respectively.

data treatment, the amplitude data is proportional to the absorption of the probe beam in the propagation through the crystal, and the phase data to the dispersion-induced dephasing. This last information is suitable as an error signal for a servo loop locking the slave laser optical frequency onto the central frequency of the narrow spectral hole.

The error signal is then processed in a digital proportional and double integrator corrector before generating frequency corrections applied to the master/slave offset phase lock used to maintain the slave laser at resonance with the spectral hole. The overall lock bandwidth is limited in practice to about 50 Hz by the delay time accumulated in transferring data between the FPGA and the computer, including the computer's timing lag, as well as the necessary processing time.

5. Effect of the servo loop

The servo loop ensures that the optical frequency of the slave laser remains at resonance with the spectral hole. By means of frequency comparison with a state-of-the-art ultrastable laser [30] via an optical frequency comb [31], we can characterize the frequency evolution of the slave laser, when the servo is engaged or not. The laser frequency locked to a single spectral hole exhibits a fractional frequency stability in the low 10^{-14} from 1 to 100 s timescales, a substantial improvement over the laser only pre-stabilized to the reference cavity (see Fig. 4). This is a proof-of-principle demonstration of our frequency locking method and technique. We have successfully operated the lock over 12 hours, only interrupted voluntarily. As in the work of Leibrandt and Cook et al. [22, 23], we observe a degradation of the locked stability when operating continuously for several hours. This is due to progressive over-burning of the spectral hole by the slave laser, even though the optical power is reduced to 100 nW for a 0.5 cm^2 beam cross-section. Indeed, after 1 h of operation, the spectral hole linewidth increased to 20 kHz. We have not yet implemented a repumping mechanism as done in the work of Cook et al. [22], but such mechanism is compatible with our interrogation method and setup, and we expect similar results with such scheme implemented, *i.e.* after a few hours to reach a steady state capable of persisting indefinitely without degradation.

6. Discussion

In the current implementation, the final instability is imposed for a large part by the detection noise, and not the crystal itself. Indeed, detection noise on the relative phase measurement from

Optics EXPRESS

the beatnotes in PD1 and PD2 produces a frequency instability when the laser is locked to a spectral hole, with a conversion factor equal to the slope of the dispersion curve around the center of the hole. Assuming a hole with a Lorentzian lineshape (FWHM denoted $\Delta\nu$) and a depth D (given by the ratio between the transmitted power at the center of the hole and transmitted power away from the hole), applying the Kramers-Kronig relation leads to a discriminator slope of $\ln(D)/\Delta\nu \simeq 0.2$ mrad.Hz^{-1} (for $D = 2.5$ and $\Delta\nu \simeq 4$ kHz in our case), a value that we confirmed experimentally (before over-burning occurs). A first indication that the detection noise constitutes a limitation comes from the fact that overburning of the spectral hole (which broadens the hole and therefore reduces the slope of the frequency discriminator) leads to a decrease of the frequency stability of the laser over time. We further confirm this by measuring the instability of the phase detection in the absence of a crystal which, when taking into account the experimental slope of the discriminator, is sufficient to explain the instability of the locked laser. Further work will be devoted to improving this phase measurement stability by improving the RF frequency chain and noise of the analog to digital conversion, as well as reducing the hole linewidth by reducing the temperature and the residual mechanical vibrations of the cryostat.

Ultimately, the detection noise would be limited by shot-noise, thermal noise and quantization noise in the ADC. For a 100 nW slave and 1 mW master lasers applied to the crystal, with typical amplified silicon pin photodiodes and 50 ohms impedance matched amplification and demodulation chain, considering the 14 bits 200 MSPS ADC of the SDR platform, we estimate that the thermal noise would be the dominant effect (unless using cryogenic photodetectors and preamplifiers, or possibly very low noise avalanche photodiodes). The thermal noise-induced limit (calculated from the specified Noise Equivalent Power of the EOT2030A photodiodes in use) would result in a white phase detection noise of -102 dBc/Hz (assuming uncorrelated thermal noise contributions from the two detectors). When probing a single hole with a 0.2 mrad.Hz^{-1} discriminator, this implies a frequency noise limit of about -28 dB(Hz^2)/Hz, *i.e.* a relative frequency stability of about $6 \times 10^{-17}\tau^{-1/2}$ for a time constant τ expressed in seconds. Probing several identical holes in parallel, each with 100 nW, would improve this limit proportionally to the square root of the number of holes. With the current setup, probing >100 holes appears feasible, with a maximum number set by the ratio between the hole linewidth and the Nyquist bandwidth of, currently, 1 MHz. Also, reducing the linewidth of the hole(s) would improve proportionally the thermal noise-induced fractional frequency stability limit.

Our fully digital heterodyne implementation allows to easily scale up the number of holes probed in parallel to such a large number. By increasing the number of holes probed in parallel while maintaining the *total* optical probe power constant, the optical power per hole is reduced, and the effect of overburning is decreased. We have qualitatively confirmed this experimentally for a few holes probed in parallel. Alternatively, by keeping the power *per hole* constant, the shot and thermal noise limit to the signal-to-noise ratio would decrease (in this case without reduction of overburning effects). We believe this alternative strategy will be useful in future work, but will first require improving other technical noise sources before being put to use.

The locking bandwidth of the system is currently limited to a few tens of Hz by the delay time associated to data transfer between the FPGA and the computer, and the processing time. A substantial improvement could be obtained by transferring part or the totality of data treatment to the FPGA, thereby reducing lag time and increasing calculation speed. However, this would be at the cost of fast and easy prototyping, as modifying data treatment in the GNU Radio framework simply corresponds to modifying a few lines of Python or C++ programing, without the complexity and long compilation times needed for reprogramming an FPGA.

7. Conclusion

We have made a proof-of-principle demonstration of a novel locking technique allowing to servo the frequency of a laser onto a narrow spectral hole previously photo-imprinted in a

Optics EXPRESS

rare-earth doped crystal at cryogenic temperature. The technique uses dispersive probing of the spectral holes and heterodyne digitization of beatnotes to deduce an error signal by a complex data processing flow. The data processing is realized in an FPGA and a computer, using an open-source software defined radio framework, that allows easy and fast prototyping with Python and/or C++. We have shown that this technique allows improving the frequency stability of a laser pre-stabilized to a Fabry-Perot cavity. In the current system, a fractional frequency stability in the low 10^{-14} from 1 to 100 s is obtained.

The current setup will need improvement in terms of detection noise and locking bandwidth, but constitute a good test-bed for future developments towards the goal of realizing an ultra-high frequency stability laser suitable for probing optical lattice clocks near their quantum projection noise limit. In particular, assuming we can reach thermal-noise limited photodetection, and probe in parallel 500 spectral holes (each of 1 kHz linewidth) with a total optical power applied to the crystal of 500 $\times$ 100 nW=50 μW for the slave laser and 1 mW for the master laser, the detection noise would lead to a fractional frequency stability at τ seconds of $\simeq 6 \times 10^{-19}\tau^{-1/2}$ (notwithstanding the intrinsic stability of the crystal). This is well below any current requirements within the field of atomic clocks and beyond. Furthermore, we are convinced that the heterodyne interrogation method and digital data processing procedure we describe is of interest in a larger variety of applications exploiting narrow structures in rare-earth doped crystals or other systems. For instance, nano-scale mechanical resonators of rare-earth doped crystals have recently been proposed for studying quantum effects [32] and the methods and setup presented in this paper could prove valuable in this context.

Funding

Ville de Paris Emergence Program, First-TF Labex, Région Ile de France; European Union's Horizon 2020 research and innovation program under grant agreement No 712721 (NanOQTech); ANR under grant number 14-CE26-0037-01 DISCRYS; EMPIR 15SIB03 OC18 and from the EMPIR program co-financed by the Participating States; and the Alexander von Humboldt-Stiftung.

Acknowledgments

We thank Michel Lours and José Pintho for electronics support, and Sébastien Bize and Giorgio Santarelli for fruitful discussions.